DISCLAIMER

This report was prepared as an account of work sponsored by an agency of the United States Government. Neither the United States Government nor any agency thereof, nor any of their employees, makes any warranty, express or implied, or assumes any legal liability or responsibility for the accuracy, completeness, or usefulness of any information, apparatus, product, or process disclosed, or represents that its use would not infringe privately owned rights. Reference herein to any specific commercial product, process, or service by trade name, trademark, manufacturer, or otherwise does not necessarily constitute or imply its endorsement, recommendation, or favoring by the United States Government or any agency thereof. The views and opinions of authors expressed herein do not necessarily state or reflect those of the United States Government or any agency thereof. Reference herein to any social initiative (including but not limited to Diversity, Equity, and Inclusion (DEI); Community Benefits Plans (CBP); Justice 40; etc.) is made by the Author independent of any current requirement by the United States Government and does not constitute or imply endorsement, recommendation, or support by the United States Government or any agency thereof.

BNL-228083-2025-TECH

EIC-ADD-TN-121

Polarized Photocathodes development for the EIC: Optimizing Spin and Quantum Efficiency

J. Biswas

April 2025

Electron-Ion Collider

Brookhaven National Laboratory

U.S. Department of Energy

USDOE Office of Science (SC), Nuclear Physics (NP)

DISCLAIMER

Polarized Photocathodes development for the EIC: Optimizing Spin and Quantum Efficiency

Jyoti Biswas* and Erdong Wang†
Brookhaven National Laboratory, Upton, NY 11973,USA
(Dated: April 28, 2025)

GaAs/GaAsP superlattice photocathodes play a critical role for producing highly polarized electron beams for the Electron-Ion Collider (EIC) at Brookhaven National Laboratory. The electron pre-injector for the EIC requires electron bunches with high bunch charge (1-2 nC) and high polarization, from GaAs-based superlattice photocathode. Herein, we have systematically investigated a range of GaAs/GaAsP superlattice photocathodes fabricated via molecular beam epitaxy (MBE) and metal-organic chemical vapor deposition (MOCVD). Through optimization of pre-cleaning procedures and surface doping conditions, we aim to identify the most promising photocathode configurations for future EIC operations. To enhance the quantum efficiency (QE), a Distributed Bragg Reflector structure is frequently incorporated beneath the superlattice. While this approach effectively increases QE, it also introduces additional complexities that can adversely influence spin polarization and the spectral response at specific laser wavelengths. This note provides an overview of superlattice GaAs development and outlines the EIC team's ongoing efforts to address related challenges and advance high-performance photocathode development tailored for the EIC. Over five years of multi-institutional collaboration and measurements of about 50 SL-GaAs samples, our analysis presents statistics on samples exhibiting high ESP and high QE. It will help to set the initial ESP requirements for the EIC project.

I. INTRODUCTION

Polarized electron sources are crucial for various fields of fundamental research disciplines, including condensed matter physics and high-energy particle physics. The Electron-Ion Collider (EIC) requires a polarized electron beam with about 7 nC of initial bunch charge and spin polarization of at least 85% from the source in the CDR stage[1]. Recently, EIC is considering to lower the charge to 1-2 nC, while increasing the initial ESP requirements to 88%. The maximum polarization from bulk GaAs is about 35-40% due to the degeneracy of the heavy-hole and light-hole at the $2p_{3/2}$ band state and spin relaxation. GaAs/GaAsP-based superlattice layer can eliminate the degeneracy in the $2p_{3/2}$ band state, thus spin-polarized electrons can be extracted from one of the bands. Strained superlattice GaAs typically achieves a spin polarization up to 90% with a quantum efficiency (QE) of approximately 1% for specific laser wavelengths[2, 3]. Adding a Distributed Bragg Reflector (DBR) under the superlattice layer enhances photon absorption and improves the QE[4].

The GaAs/GaAsP superlattice photocathode produced by SVT Associates supported by the DOE SBIR/STIR program is recognized as a benchmark of success[4]. SVT Associates has discontinued the sale of photocathodes at about 2017. The safety and equipment hazards associated with handling flammable phosphorus, coupled with the limited market for these photocathodes, create an unfavorable scenario for commercial vendors. A major challenge for industrial leadership is that there are presently few commercial applications of polarized beams from GaAs photocathodes. The limited availability of GaAs/GaAsP superlattice photocathodes has resulted in a global "spin crisis", with no vendors currently capable of providing photocathodes that simultaneously achieve high QE and ESP. This challenge has prompted extensive collaborative efforts worldwide, involving institutions such as Old Dominion University[5], Jefferson Lab, Brookhaven National Laboratory, Sandia National Laboratories[6], and others, to revive the development of high-QE and high-ESP GaAs photocathodes. Since November 2024, major concerns have been raised by the U.S. vendors have ceased bulk GaAs production due to restrictions on gallium exports. This increased uncertainty in the supply chain of polarized photocathodes, raising operational risks for the EIC and other polarized electron facilities.

This note summarizes all the SL-GaAs samples obtained by the BNL CAD/EIC team collaborating with several MBE/MOCVD growth teams, such as from Nogoya/SVT/ODU/SandiaLab/Acken in the last four years. It provides the guidelines for the project evaluating the risks of generating the initial high polarization from the cathode.

II. SUMMARY OF R&D AND PRODUCTION GAAS CATHODE

Table I summarized all the III-V polarized photocathode structures based on authors best of knowledge. Since then, the research interests have focused on how to increase the QE. Using strained GaAs is a major step of increasing the polarization. Since then, the research interests have focused on how to increase the QE.

* jbiswas@bnl.gov
† wange@bnl.gov

TABLE I: Comparison of various SL-GaAs photocathodes

Photocathode	**Institute**	**ESP (%)**	**QE (%)**	**HH-LH splitting (meV)**	**Growth method**	**Ref**	**Note**
$GaAs/Al_{0.35}GaAsAl_{0.35}GaAs$ buffer	Nagoya	71.2	NA	44	MBE	PRL 67, 3294 (1991)	Strain is very small
GaAs single layer$GaAsP_{0.12}$ buffer	Nagoya	80	1	NA	MOVPE	JJAP 32, L1837 (1993)	$Al_{0.1}GaAs/Al_{0.6}GaAs$ First DBR sample
$In_{0.15}GaAs/GaAsAl_{0.4}GaAs$ buffer	Nagoya	82.7	0.015	70	MBE	JJAP 33, 5676 (1994)	
AlInGaAs single layerAlGaAs buffer	St. Peterburg	80	NA	NA	MOCVD	PRL 74, 2106 (1995)	GaAs/AlGaAs DBR
$GaAs/GaAsP_{0.36}GaAsP_{0.36}$ buffer	SVT/SLAC	86	1.2	82	GSMBE	APL 85, 2640 (2004)	Typical SSL
$In_{0.15}GaAs/Al_{0.38}GaAsAl_{0.38}$GaAs buffer	Nagoya	77	0.7	104	MBE	JAP 97, 094907 (2005)	
$GaAs/GaAsP_{0.34}GaAsP_{0.34}$ buffer	Nagoya	92	0.5	80	MBE	JAP 97, 094907 (2005)	
$Al_{0.18}In_{0.12}GaAs/GaAsP_{0.17}$$Al_{0.3}GaAs$ buffer	St. Peterburg	84	0.4	40	MOVPE	APL 86, 171911 (2005)	Strain compensated
$Al_{0.25}In_{0.27}GaAs/GaAsAl_{0.35}$GaAs buffer	St. Peterburg	88	0.57	77	MBE	Semi. 40, 1326 (2006)	
$Al_{0.19}In_{0.2}GaAs/Al_{0.4}GaAsAl_{0.4}GaAs$ buffer	St. Peterburg	92	0.85	87	MBE	APL 93, 081114 (2008)	
$GaAs/GaAsP_{0.38}Al_{0.1}GaAsP_{0.19}$ buffer	Nagoya	92	1.6	89	MOVPE	APL 15, 203509 (2014)	Strain compensated
$GaAs/GaAsP_{0.35}GaAsP_{0.35}$ buffer	SVT/JLab	84	6.4	81.2	SSMBE	APL 109, 252104 (2016)	GaAsP/AlAsP DBR
$GaAsSb_{0.147}/Al_{0.38}GaAsAl_{0.38}GaAs$ buffer	SVT/JLab	75	0.62	132	SSMBE	AIP Adv. 8, 075308 (2018)	
$GaAs/GaAsP_{0.38}GaAsP_{0.19}$ buffer	BNL/Sandia	70	15	89	MBE	AIP Advances 13, 085106 (2023)	Strain compensated, GaAsP/AlAsP DBR
$GaAs/GaAsP_{0.35}GaAsP_{0.35}$ buffer	JLab/BNL/ODU	84(92 unpub)	2.8	81.2	MOCVD	APL, 123, 222102 (2023)	GaAsP/AlAsP DBR
$GaAs/GaAsP_{0.35}GaAsP_{0.35}$ buffer	JLab/UCSB	–	–	–	CBE	In process	
GaAsSb/AlGaAsAlGaAs buffer	BNL/SBU	–	–	–	MBE	Proposed	AlGaAsSb/AlAsSb DBR (declined)

The ESP remains below 92% and most of the cases are about 85%, fundamentally limited by the depolarization mechanisms such as D'yakonov-Perel (DP) mechanism and Bir-Aronov-Pikus mechanism [7, 8]. In all reported structures, the strained GaAs/GaAsP superlattice grown on GaAsP buffer layer has the best performance and the most widely used. The strained AlInGaAs/AlGaAs superlattice grown on AlGaAs buffer layer also exhibits high ESP similar to GaAs/GaAsP photocathode. The strained GaAsSb/AlGaAs superlattice has the highest heavy-hole and light-hole (HH-LH) splitting energy, which is expected to give the highest ESP, but has not been successful.

Three semiconductor growth methods are used to grow the GaAs-based photocathodes: MBE, MOCVD, and Chemical beam epitaxy (CBE). MBE and MOCVD have been successful in growing high-polarization GaAs-based photocathodes, both achieving high performance. CBE is a new proposed method to grow GaAs-based photocathodes.

MBE is an epitaxy method for thin-film deposition of single crystals. Molecular-beam epitaxy takes place in high vacuum or ultra-high vacuum (10^{-8} to 10^{-12} Torr). The most important aspect of MBE is the deposition rate (typically less than 3,000 nm per hour) that allows the films to grow epitaxially. These deposition rates require proportionally better vacuum to achieve the same impurity levels as other deposition techniques. The absence of carrier gases, as well as the ultra-high vacuum environment, results in the highest achievable purity of the grown films. MBE includes gas source MBE (GSMBE) and solid source MBE (SSMBE). In solid source MBE, elements such as gallium and arsenic, in ultra-pure form, are heated in separate quasi-Knudsen effusion cells or electron-beam evaporators until they begin to sublime slowly. The gaseous elements then condense on the wafer, where they may react with each other. Controlling the temperature of the source will control the rate of material impinging on the substrate surface and the temperature of the substrate will affect the rate of hopping or desorption. The term "beam" means that evaporated atoms do not interact with each other or vacuum-chamber gases until they reach the wafer, due to the long mean free paths of the atoms. In GSMBE, group-III species are elemental sources, while the group-V ones are hydrides, such as arsine (AsH_3), phosphine (PH_3), and stibine (SbH_3), that are admitted to the UHV growth chamber and then thermally cracked by contact with hot surfaces in suitable cells to generate dimer beams.

MOCVD, also known as organometallic vapor-phase epitaxy (OMVPE) or Metalorganic vapor-phase epitaxy (MOVPE), is a chemical vapor deposition method used to produce single- or polycrystalline thin films. It is a process for growing crystalline layers to create complex semiconductor multilayer structures. In contrast to molecular-beam epitaxy (MBE), the growth of crystals is

by chemical reaction and not physical deposition. This takes place not in a vacuum, but from the gas phase at moderate pressures (10 to 760 Torr). As such, this technique is preferred for the formation of devices incorporating thermodynamically metastable alloys, and it has become a major process in the manufacture of optoelectronics, such as Light-emitting diodes, or solar cells.

CBE forms another important class of deposition techniques for semiconductor systems, especially III-V semiconductor systems. This form of epitaxial growth is performed in an ultrahigh vacuum system. The reactants are in the form of molecular beams of reactive gases, typically as the hydride or a metalorganic. The term CBE is often used interchangeably with metal-organic molecular beam epitaxy (MOMBE). The nomenclature does differentiate between the two (slightly different) processes, however. When used in the strictest sense, CBE refers to the technique in which both components are obtained from gaseous sources, while MOMBE refers to the technique in which the group III component is obtained from a gaseous source and the group V component from a solid source.

III. EIC MINI MOTT POLARIMETER

Photocathode samples were evaluated within a low-voltage retarding-field Mott polarimeter located at EIC, BNL. Mott polarimeters utilize the left-right scattering asymmetry arising from spin-orbit coupling when high-energy electrons are scattered at large angles off a high-Z target. A layout of this Mott polarimeter system is shown in Fig. 1. The system consists of a load lock manipulator, a cathode activation chamber, and a Mott detector. The base pressure of the activation chamber is 10^{-11} Torr. Samples are activated at room temperature to form a negative electron affinity (NEA) surface using the alternate deposition of Cs and O_2, commonly known as "yo-yo" activation. The QE of the samples could be measured using a circularly polarized laser with a wavelength ranging from 700 to 800 nm. Circularly polarized light was generated using a linear polarizer, a quarter-wave plate, and a polarizing beam splitter cube, and was directed onto the sample to generate spin-polarized electrons.

The electron spin vector **S** is longitudinal and does not change in an electrostatic field. An electrostatic 90° deflector converts a longitudinal spin component into a transversal one. Following the 90° deflection, the electron beam passes another scattered electron repeller, and the electrons enter the spin detector. On entering the spin detector, electrons are accelerated up to 25 kV. They are then scattered at the thorium target and then pass a focus electrode in front of each channel electron multipliers (CEMs). After passing the focus electrode, the electrons are retarded by a grid in front of the CEM. The spin grid voltage defines the detector window for inelastic scattering. The electrons scatter from the thorium target and, after decelerating to almost ground potential, they are detected by CEMs in the Mott detector. Each CEM pairs determine spin direction using so called asymmetry function, defined as the signal intensities from opposing channels. Asymmetry, $A = (S_1 - S_2)/(S_1 + S_2)$ with S_1 and S_2 are the signal intensities from each channel. The spin polarization, P is calculated according to $P = A/S_{eff}$, where S_{eff} is the effective Sherman function. In our case, the effective Sherman function was 0.27 ± 0.006, obtained from measurements of bulk GaAs, assuming a known polarization of 35%. Laser polarization was assumed to be 100%; later measurements showed 97%, but this was not taken into account in the polarization calculation.

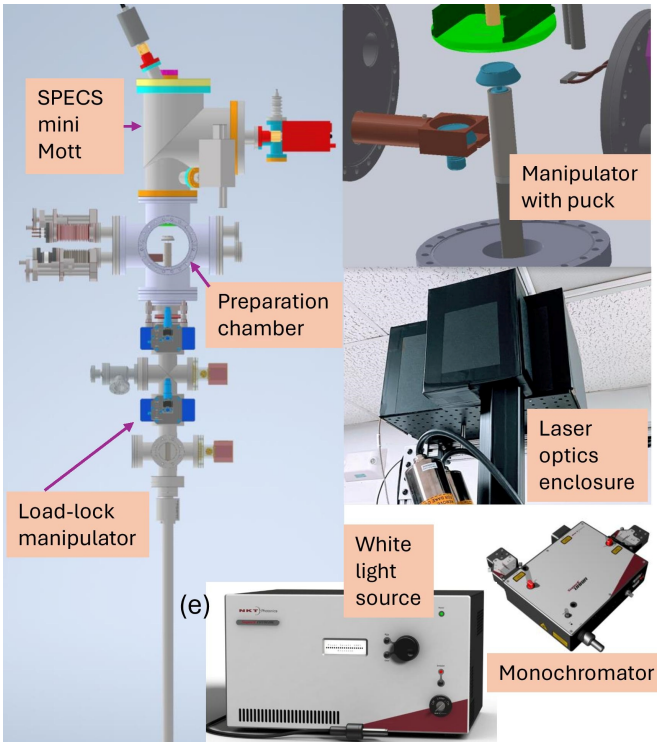

FIG. 1: Layout of the Mott polarimeter system, along with load-lock manipulator, cathode activation chamber, and laser optics setup.

IV. MBE-GROWN CATHODE TESTS

Molecular-beam epitaxy (MBE) is a widely used method for the deposition of single-crystal thin films, conducted under ultra-high vacuum conditions (10^{-8} to 10^{-12} Torr). A key characteristic of MBE is its low deposition rate, which is essential for promoting epitaxial film growth. These low rates demand a substantially higher vacuum quality than other deposition methods to achieve comparable impurity levels. The absence of carrier gases, coupled with the ultra-high vacuum environment, enables the fabrication of films with exceptional purity.

Acken Optoelectronics Ltd. from China, has started

production of GaAs/GaAsP photocathodes using MBE system. At the same time, Sandia National Laboratories started growing MBE-grown samples, which we have tested in our mini Mott at BNL.

A. Acken MBE-grown samples

We have made a purchase order with Acken Optoelectronics Ltd. China to provide us initially with six GaAs photocathodes. The structure of the MBE-grown GaAs sample is depicted in Table II. Top 5 nm is doped with Zn, and the doping density is $5 \times 10^{19}/cm^3$.

Layer	Thickness	Doping (p-type)
GaAs	5 nm	5×10^{19} cm^{-3}
GaAs/GaAsP SL	(3.8/2.8 nm) ×14	5×10^{17} cm^{-3}
$GaAsP_{0.35}$	2750 nm	5×10^{18} cm^{-3}
Graded $GaAsP_x$ (x=0∼0.35)	5000 nm	5×10^{18} cm^{-3}
GaAs buffer	200 nm	2×10^{18} cm^{-3}
p-GaAs substrate ($> 10^{18}$ cm^{-3})		

TABLE II: Structure of MBE-grown GaAs/GaAsP superlattice photocathodes from Acken Optoelectronics Ltd. China.

1. *Surface scratches*

When we opened the first sample (#BS2201), we observed very rough scratches on the surface. We subsequently opened other Acken samples and found similar scratches. We have measured #BS2201 and #BS2203 in the Mott system. The remaining samples show extensive surface scratching, which could adversely affect the operation or safety of the Mott polarimeter.

2. *Polarization and QE results*

The provided Acken samples have an arsenic capping layer; therefore, a heat cleaning temperature of around 500°C is sufficient to completely remove the capping layer. We followed standard heat cleaning (530°C for two hours) and activation process as follows:

- Heat-clean the sample at 530°C for two hours
- Yo-Yo activation with Cs and O_2
- Spectral response of the activated photocathode
- Electron spin polarization measurement
- Further heat clean and repeat the procedure.

Compared to the six samples received from Acken, samples #BS2201 and #BS2203 exhibited relatively fewer scratches at the center of the wafer, and we tested both samples in the Mott system. For both Acken samples, we followed the standard heat cleaning procedure (530°C for two hours), and the activation process is described above. However, the samples from Acken Ltd did not meet the requirements. Even though Acken Ltd has agreed to troubleshoot their MBE system to address the issue; however, this procurement was terminated due to big uncertainty.

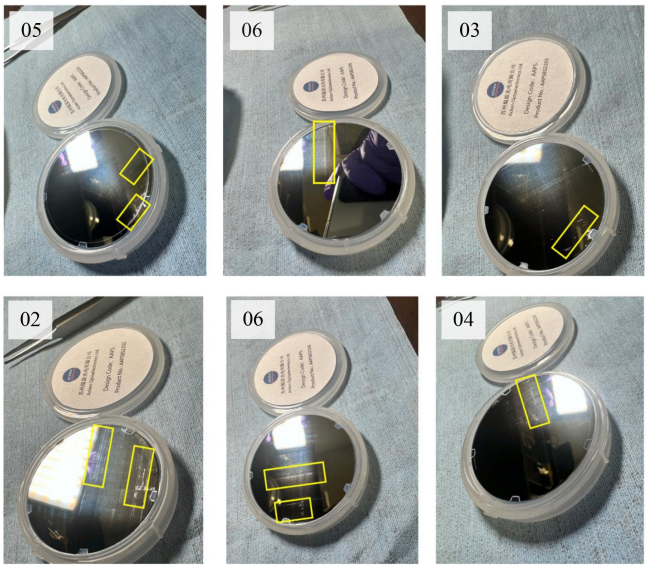

FIG. 2: All the Acken sample shows surface scratches at various positions. Samples are named as BS220X, with X = 1, 2, 3, 4, 5, 6.

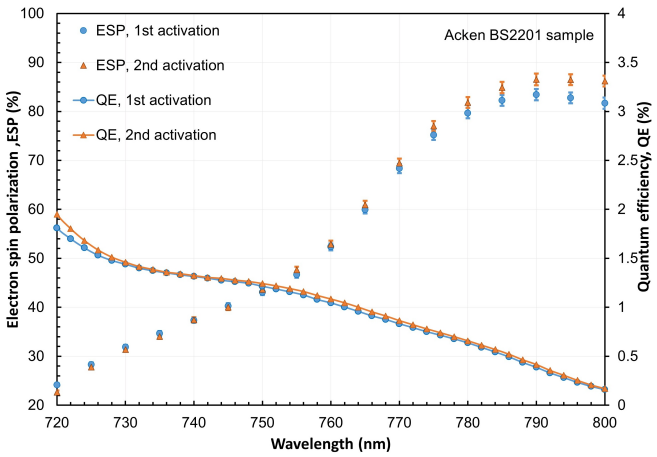

FIG. 3: The QE and electron-spin polarization for the superlattice GaAs/GaAsP (#BS2201) as a function of the wavelength, measured at away from the center of the 3-inch wafer. At around 780 nm, the polarization is just over 80% and QE is 0.7%.

B. Sandia Laboratories MBE-grown samples

To improve the QE of GaAs/GaAsP superlattice photocathode, Sandia National Laboratories has started growing a distributed Bragg reflector (DBR) grown underneath the SL with a buffer medium layer, which creates a Fabry–Pérot resonator that effectively traps the light and enhances the QE. The superlattice structure is similar to that described in table II with $GaAs_{0.62}P_{0.38}$ and $GaAs$ each having a thickness of 4 nm in the SL layer, and a total of 30 SL pairs were utilized. The DBR consists of alternating layers of high (n_H) and low (n_L) index of refraction material. The high refractive index layer is $GaAs_{0.81}P_{0.19}$ and low refractive index layer is $AlAs_{0.78}P_{0.22}$. The DBR layer consists of 10 pairs of $GaAs_{0.81}P_{0.19}$ and $AlAs_{0.78}P_{0.22}$ having thickness of 65 nm and 55 nm, respectively, as shown in Table III. The very top 5 nm GaAs was highly carbon doped with a doping concentration of $5\times10^{19}/cm^3$. Samples were terminated with an arsenic capping layer to prevent oxidation of the surface. The details of the structure of Sandia GaAs samples can be found elsewhere[6].

1. *Polarization and QE results*

We have activated and measured the spectral response and electron spin polarization in EIC mini Mott polarimeter. The samples were heated to 500°C in the preparation chamber for 2 hours to remove the arsenic capping layer and contamination from the surface under the vacuum pressure of 10^{-11} Torr scale. Samples were activated at room temperature to form a negative electron affinity (NEA) surface using the alternate deposition of cesium and oxygen. Fig. 4 shows one of the best-performing Sandia MBE-grown samples with QE of around 19% at around 774 nm with ESP just below 70%. All the Sandia samples we have tested so far had polarization below 70% and relatively high QE ranging from 10-19%. Although the Sandia samples have the highest QE reported so far at photon energies near the GaAs bandgap, the polarization being less than 70% makes them unsuitable for use in the EIC.

V. MOCVD-GROWN CATHODE TESTS

To revive the supply of superlattice GaAs/GaAsP photocathode, Old Dominion University, in collaboration with Rochester Institute of Technology, have started producing BDR-based photocathodes in a MOCVD system. ODU has been fabricating photocathodes with a structure similar to the one produced earlier by SVT. The schematic structure of the MOCVD-grown samples is depicted in Table IV. The top 5 nm of GaAs is p-doped with carbon with a carrier concentration of around $5\times10^{19}/cm^3$, and the rest of the GaAs/GaAsP layers are doped with zinc.

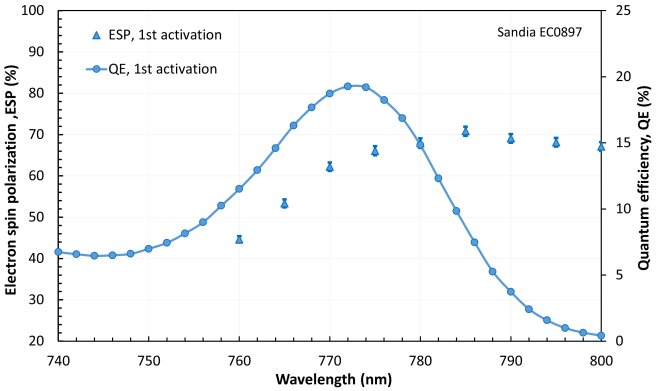

FIG. 4: The QE and electron-spin polarization for the GaAs/GaAsP superlattice DBR photocathode (#EC0897) as a function of the wavelength. Peak QE of 19% occurs at 774 nm laser wavelength, with electron spin polarization just below 70%.

A. Optimizing pre-cleaning

GaAs/GaAsP-based superlattice photocathodes grown in an MBE system are usually terminated with an arsenic capping layer, which is removed in a UHV environment by heating at an elevated temperature. In an MOCVD system, it is rather challenging to incorporate an arsenic capping layer. As a result, GaAs, when exposed to air during handling and installation, can create oxide layers, and in general, both Ga and As oxides are created. Heat treatment of around 580°C in UHV usually completely gets rid of all the oxides from the surface. However, heat treatment at around 580°C seems to cause inter-layer material diffusion as we observed in Transmission Electron Microscopy (TEM)[9].

We wanted to verify if high-temperature heat treatment, such as 580°C could cause any reduction in the doping density of the surface layer. The top 5 nm of GaAs/GaAsP superlattice layer is highly ($\sim 10^{19}/cm^3$) p-doped either using Zn or C as the dopant. TEM is not very suitable for GaAs/GaAsP doping analysis since the density of GaAs is $4.5\times10^{22}/cm^3$ and a high doping level is only incorporated in the top 5 nm. The sample under discussion is doped with carbon in the first 5 nm, and the rest of GaAs/GaAsP layers are doped with zinc. To study doping density in the surface layer, we have utilized Secondary Ion Mass Spectroscopy (SIMS). Fig. 5 shows carbon count per 10k total ions for both the pristine sample and the sample from the same wafer after 580°C heat treatment. To avoid background carbon count, we have utilized a GaAs sample with no carbon doping as our sample for background correction. Fig. 5 clearly shows that high-temperature treatment of around 580°C has adverse effects on the surface layer doping density.

To reduce the heat cleaning temperature, we have incorporated a wet cleaning method before the sample installation into the vacuum system. We immersed the

Layer	Thickness	Doping Level (p)
GaAs	5 nm	$p = 5 \times 10^{19}$ cm^{-3}
GaAs/$GaAs_{0.62}P_{0.38}$ (30 pairs)	4/4 nm	$p = 5 \times 10^{17}$ cm^{-3}
$GaAs_{0.81}P_{0.19}$	300 nm	$p = 5 \times 10^{18}$ cm^{-3}
$AlAs_{0.78}P_{0.22}$/$GaAs_{0.81}P_{0.19}$ (10 pairs)	65/55 nm	$p = 5 \times 10^{18}$ cm^{-3}
$GaAs_{0.81}P_{0.19}$	2000 nm	$p = 5 \times 10^{18}$ cm^{-3}
GaAs → $GaAs_{0.81}P_{0.19}$	2750 nm	$p = 5 \times 10^{18}$ cm^{-3}
GaAs buffer	200 nm	$p = 5 \times 10^{18}$ cm^{-3}
GaAs substrate		$p > 1 \times 10^{18}$ cm^{-3}

TABLE III: Layer structure and doping concentrations of MBE-grown BNL/Sandia sample.

Layer	Thickness	Doping (p-type)
GaAs	5 nm	5×10^{19} cm^{-3}
GaAs/GaAsP SL	(3.8/2.8 nm) ×14	5×10^{17} cm^{-3}
$GaAs_{0.65}P_{0.35}$	750 nm	5×10^{18} cm^{-3}
GaAsP/AlInP DBR layer	(54/64 nm) ×12	5×10^{17} cm^{-3}
$GaAs_{0.65}P_{0.35}$	2500 nm	5×10^{18} cm^{-3}
Graded $GaAsP_x$ (x=0∼0.35)	6000 nm	5×10^{18} cm^{-3}
GaAs buffer	500 nm	2×10^{18} cm^{-3}
p-GaAs substrate ($> 10^{18}$ cm^{-3})		

TABLE IV: Structure of MOCVD-grown GaAs/GaAsP superlattice DBR photocathodes produced in collaboration with Old Dominion University and Rochester Institute of Technology.

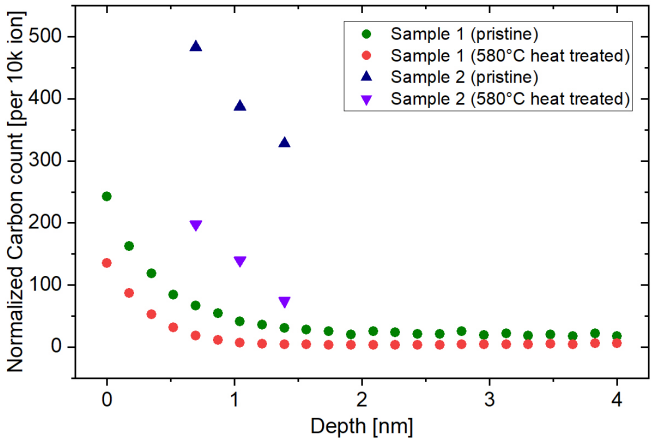

FIG. 5: SIMS cross-sectional profile for MOCVD-grown pristine sample, and sample from the same wafer after it went through two heat cleaning cycles at 580°C. Both for samples 1 and 2, we observed a reduction of carbon count in the surface layer[9].

MOCVD-grown GaAs samples in a 36% purified hydrochloric acid solution for 45 seconds, dipped into deionized water, and followed by blowing them with high-purity dry N_2 for a few seconds, then promptly installing them into the cathode puck (with Indium foil underneath for ohmic contact) and loaded into the chamber through the load-lock manipulator that was baked at 200°C for 72 hours.

B. Polarization and QE results

The MOCVD-grown GaAs sample was activated at room temperature in the preparation chamber of the Mott polarimeter to form a negative electron affinity (NEA) surface using the standard yo-yo activation procedure with Cs and O_2. Fig. 6 shows the spectral response and spin polarization of a superlattice DBR photocathode. At the center of the wafer, the peak QE wavelength position is close to the intended design value of approximately 780-785 nm. However, the peak QE position varies as we move from the center towards the edges of the wafer. Our study revealed a shift in peak QE wavelength from 770 nm to 790 nm across a 2-inch sample, indicating non-uniformity in the DBR layer across the sample, possibly due to non-uniform heating during the growth process in the MOCVD system.

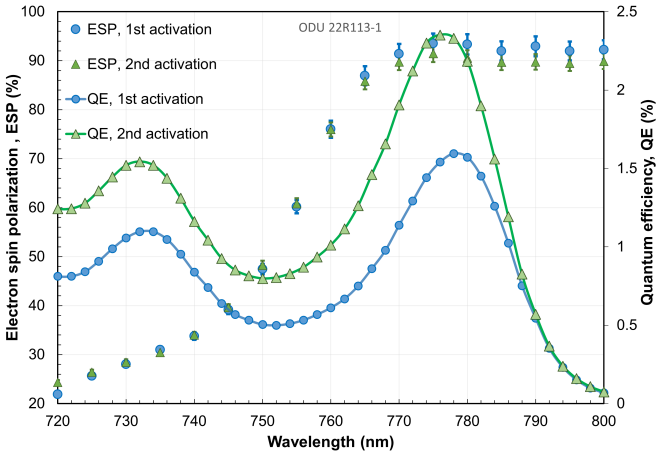

FIG. 6: The QE and electron-spin polarization of one of the best ODU MOCVD-grown GaAs/GaAsP superlattice DBR photocathode as a function of the laser wavelength, measured at nearly identical location.

In our current study, involving MOCVD samples, we have used a reduced heat treatment temperature

of 450°C, which is sufficient enough to remove most of the Arsenic oxides from the surface. Though high-temperature heat treatment of around 580°C is able to achieve a contamination-free surface and shows high QE[10], our motivation was to minimize the dopant diffusion at the surface layer so that high bunch charge could be extracted from the cathode in High Voltage Direct Current (HVDC) gun[11]. We found that in terms of achieved polarization from the SL-DBR cathode, there is no difference between 450°C and 580°C heat treatment.

C. Optimize surface doping and DBR pairs

The top 5 nm of the GaAs/GaAsP superlattice layer are usually terminated with highly p-doped material (i.e., zinc or carbon) so that it helps lower the work function, as well as prevent recombination of electrons and holes, making a net increase of emitted electrons from the cathode. Carbon as a dopant has a relatively lower diffusion rate, and hence it was a choice of dopant in our case for the surface layer.

To optimize the surface doping concentration, we tested four DBR superlattice GaAs samples with surface doping levels ranging from 1×10^{19} to 2×10^{20} $/cm^3$. The peak polarization starts to decline beyond $5\times10^{19}/cm^3$ due to the scattering of doping atoms with polarized electrons, leading to polarization degradation. Lower doping levels typically yield higher spin polarization, whereas higher surface doping helps suppress the surface charge effect while extracting electron beam in a gun. Considering the figure of merit (P^2QE) of the polarized source, where P represents polarization, achieving high polarization is the most crucial factor. Therefore, based on this criterion, we determine to use the sample with the highest figure of Merit, which has the optimal surface doping level of $5\times10^{19}/cm^3$.

A sample with an optimal surface doping of $5\times10^{19}/cm^3$ underwent pre-cleaning with HCL and a reduced heat treatment temperature of around 450°C in UHV. Subsequently, it was activated and tested in HVDC electron gun[11]. The HVDC gun was operated at 300 kV, and the test of the SL-DBR cathode in the HVDC gun shows that a lower heat cleaning temperature of 450°C (compared with traditional 580°C heat treatment) helps to suppress the surface charge effect. Details of this study will be discussed elsewhere.

To optimize the number of DBR pairs, we have utilized samples with varied DBR pairs, ranging from 12, 16, and 20 pairs. The DBR pair is composed of alternate layer of $GaAs_{0.65}P_{0.35}$ and $In_{0.30}Al_{0.70}P$. The DBR pairs were Zn doped with a doping density of $5\times10^{18}/cm^3$. The very surface carbon doping of all these samples was close to $5\times10^{19}/cm^3$. The main purpose of the DBR layer is to increase the absorption of photons in GaAs at a desired wavelength. However, having too many DBR layers could increase the cavity Q factor, causing a smaller bandwidth and a drop in QE. Fig. 7 shows a comparison of the figure of merit (P^2QE) for different DBR pair numbers with respect to wavelength. A higher figure of merit was achieved for the sample with 16 DBR pairs.

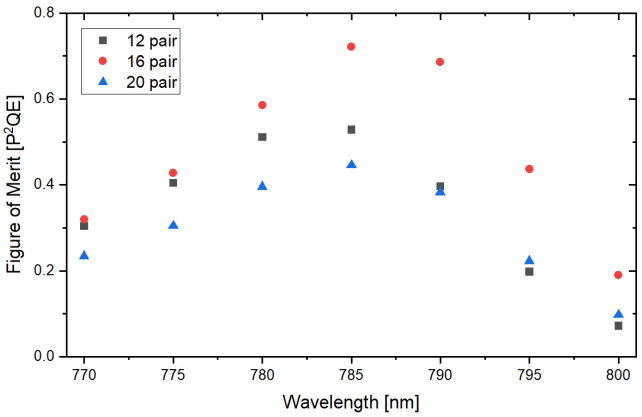

FIG. 7: Figure of merit (P^2QE) for ODU MOCVD-grown superlattice DBR samples with a varied number of DBR pairs.

VI. INSIGHTS FROM ALL THE TEST RESULTS

In our EIC mini Mott polarimeter, we have evaluated spectral response and electron spin polarization for over 50 photocathodes. Six important categories include: (a) MBE-grown SVT associates photocathodes, (b) MBE-grown Sandia Laboratories photocathodes, (c) MBE-grown China Acken photocathodes, (d) MOCVD-grown ODU photocathodes, (e) MBE-grown Nagoya photocathode, and (f) MOCVD-grown SMI Inc photocathodes. Fig. 8 shows an insight into the QE and ESP of all the photocathodes tested in the Mott system. Cathodes having ESP below 60% or QE peak position too far from the near bandgap photon energies are omitted in this plot. To compare photocathodes from different institutions/industry, we did not use the term figure of merit (P^2QE), which is typically used in the target experiment. In the storage ring collider, the polarization decay is dominated by the Sokolov-Ternov effect and depolarization by diffusion. Meanwhile, the current is limited by the storage ring as well. The initial electron source current is not important, however, the electron source polarization will determine the storage ring polarization decay initial value. Therefore, a high ESP of electron source is essential. For example, MBE-grown Sandia photocathodes have the highest QE as well as the highest figure of merit (P^2QE), however, the polarization is always below 70%, making it not a suitable choice for the EIC. MBE-grown China Acken samples have polarization between 80-85% with acceptable QE; however, the surface scratches, lack of reproducibility create uncertainty in future production. SVT MBE-grown samples are standard, but they shut down the production long ago. ODU tried to rescue

with MOCVD-grown samples; however, still in the process of tweaking the growth recipe to make reproducible results. Similarly, SMI is still tweaking their MOCVD growth recipe to make a reproducible photocathode.

It is clear that achieving reproducible SL-GaAs samples with both high QE and high ESP remains very challenging. In particular, DBR samples require precise resonance wavelength tuning, making it nearly impractical to consistently produce high-quality samples. One potential approach for the EIC is to utilize non-DBR regular SL-GaAs samples. However, the higher QE of DBR samples does offer the project valuable headroom for generating high bunch charge beams. The polarization requirement for the EIC electron source has increased from 80% in the CDR stage to a tentative 88%, raising the risk associated with polarized source production due to observing higher spin loss in the RCS and storage ring. We suggest setting a target of 85% polarization to better manage and control the associated risks.

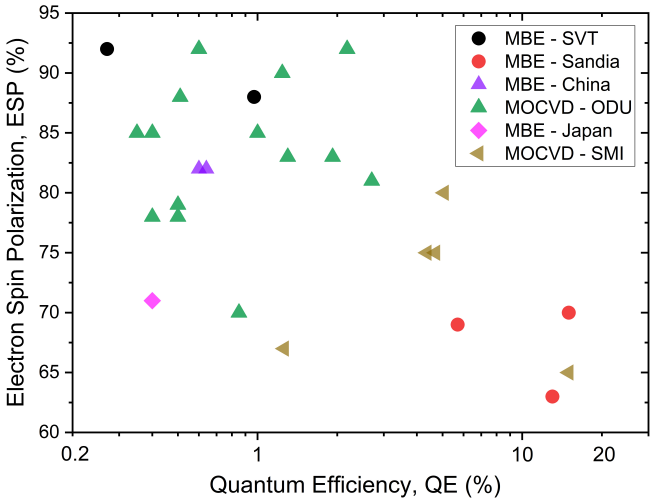

FIG. 8: Evaluation of QE and spin polarization from various MBE and MOCVD-grown superlattice GaAs photocathode at EIC mini Mott system. Cathodes having ESP below 60% or QE peak position too far from the near bandgap photon energies are omitted in this plot.

VII. SUMMARY AND FUTURE OUTLOOK

We have been in close collaboration with multiple institutions and industry to hunt for a suitable photocathode that satisfies high polarization with acceptable QE (>0.8%), and has reproducibility. So far, Sandia MBE-grown samples, as well as China MBE-grown GaAs samples, have not met the requirements. We have tested a wide range of ODU MOCVD-grown samples and identified the doping concentration and cleaning procedures necessary for the new MOCVD-grown GaAs samples. ODU has opted to manufacture additional samples with enhanced or at least acceptable ESP as set for the EIC requirements. Over the next 4-5 years, the received samples will undergo measurement in the Mott polarimeter, allowing us to assess spin polarization, quantum efficiency, and photocathode lifetime. If these evaluations demonstrate satisfactory performance, we plan to reserve a significant portion of the samples for future utilization in the EIC project. To ensure their preservation, we have designated a dedicated vacuum storage chamber for crucial samples. We are actively engaging with other potential vendors who may be interested in developing this type of photocathode with support from the DOE.

VIII. ACKNOWLEDGE

We thank our collaborators Adam Masters, Sylvain Marsillac, and Matt Poelker for their contributions to the study of MOCVD-grown GaAs/GaAsP photocathodes. We also thank Luca Cultrera for providing the GaAs/GaAsP photocathode in collaboration with Sandia National Laboratories and SMI Inc. Additionally, we thank our former colleague Wei Liu for commissioning the Mott system and performing the initial measurements.

[1] E. Wang, J. Skaritka, J. Biswas, and V. Ranjbar, The design progress of a high charge low energy spread polarized pre injector for Electron Ion Collider, JACoW, IPAC2024 , MOPC24 (2024).

[2] T. Maruyama, D.-A. Luh, A. Brachmann, J. E. Clendenin, E. L. Garwin, S. Harvey, J. Jiang, R. E. Kirby, C. Y. Prescott, R. Prepost, *et al.*, Systematic study of polarized electron emission from strained gaas/gaasp superlattice photocathodes, Appl. Phys. Lett. **85**, 2640 (2004).

[3] T. Nishitani, T. Nakanishi, M. Yamamoto, S. Okumi, F. Furuta, M. Miyamoto, M. Kuwahara, N. Yamamoto, K. Naniwa, O. Watanabe, Y. Takeda, H. Kobayakawa, Y. Takashima, H. Horinaka, T. Matsuyama, K. Togawa, T. Saka, M. Tawada, T. Omori, Y. Kurihara, M. Yoshioka, K. Kato, and T. Baba, Highly polarized electrons from gaas–gaasp and ingaas–algaas strained-layer superlattice photocathodes, J. Appl. Phys. **97**, 094907 (2005).

[4] W. Liu, Y. Chen, W. Lu, A. Moy, M. Poelker, M. Stutzman, and S. Zhang, Record-level quantum efficiency from a high polarization strained gaas/gaasp superlattice photocathode with distributed bragg reflector, Applied Physics Letters **109**, 252104 (2016).

[5] B. Belfore, A. Masters, D. Poudel, G. Blume, S. Polly, E. Wang, S. M. Hubbard, M. Stutzman, J. M. Grames,

M. Poelker, M. Grau, and S. Marsillac, High figure of merit spin polarized electron sources grown via mocvd, Applied Physics Letters **123**, 222102 (2023).

[6] J. Biswas, L. Cultrera, W. Liu, E. Wang, J. Skaritka, K. Kisslinger, S. D. Hawkins, S. R. Lee, and J. F. Klem, Record quantum efficiency from strain compensated superlattice gaas/gaasp photocathode for spin polarized electron source, AIP Advances **13**, 085106 (2023).

[7] G. Bir, A. Aronov, and G. Pikus, Spin relaxation of electrons due to scattering by holes, Zh. Eksp. Teor. Fiz **69**, 1382 (1975).

[8] M. D'yakonov and V. Perel, Spin orientation of electrons associated with the interband absorption of light in semiconductors, Soviet Journal of Experimental and Theoretical Physics **33**, 1053 (1971).

[9] J. Biswas, E. Wang, O. Rahman, J. Skaritka, K. Kim, A. Masters, S. Marsillac, and T.-D. Lee, Quest for an Optimal Spin-Polarized Electron Source for the Electron-Ion Collider, JACoW, IPAC2024 , MOPR77 (2024).

[10] J. Biswas, E. Wang, M. Gaowei, W. Liu, O. Rahman, and J. T. Sadowski, High quantum efficiency gaas photocathodes activated with cs, o2, and te, AIP Advances **11**, 025321 (2021).

[11] E. Wang, O. Rahman, J. Biswas, J. Skaritka, P. Inacker, W. Liu, R. Napoli, and M. Paniccia, High-intensity polarized electron gun featuring distributed bragg reflector gaas photocathode, Applied Physics Letters **124**, 254101 (2024).

More references are listed in the Table I